

# Solution and Solid-State Structures of Phosphine Adducts of Monomeric Zinc Bisphenoxide Complexes. Importance of These Derivatives in CO<sub>2</sub>/Epoxide Copolymerization Processes<sup>†</sup>

Donald J. Darensbourg,\* Marc S. Zimmer, Patrick Rainey, and David L. Larkins

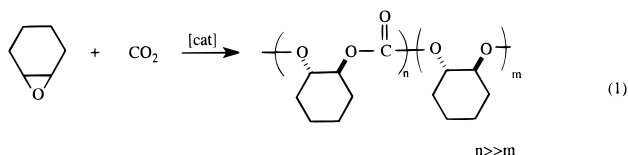
Department of Chemistry, Texas A&M University, P.O. Box 30012, College Station, Texas 77842-3012

Received May 24, 1999

Phosphine derivatives of the monomeric zinc phenoxide complexes, (phenoxide)<sub>2</sub>ZnL<sub>n</sub>, where phenoxide equals 2,6-di-*tert*-butylphenoxide, 2,4,6-tri-*tert*-butylphenoxide, and 2,6-diphenylphenoxide and  $n = 1$  or 2, have been synthesized from the reaction of Zn[N(SiMe<sub>3</sub>)<sub>2</sub>]<sub>2</sub> and the corresponding phenol followed by the addition of phosphine. The complexes have been characterized in solution by <sup>31</sup>P NMR spectroscopy and in selected instances in the solid-state by X-ray crystallography. The small, basic phosphine, PMe<sub>3</sub>, provided the only case of an isolated complex possessing two phosphine ligands (i.e.,  $n = 2$ ). For all other larger phosphines only the monophosphine adducts were obtained. Furthermore, only fairly basic phosphines were found to bind to zinc, e.g., whereas PPh<sub>3</sub> ( $pK_a = 2.73$ ) was ineffective, PPh<sub>2</sub>Me ( $pK_a = 4.57$ ) did form a strong bond to zinc. The solid-state structures of the monophosphine adducts consist of a near-trigonal planar geometry about the zinc center, where the average P–Zn–O angles are larger than the O–Zn–O angles. On the other hand, the bisphosphine adduct, Zn(O-2,4,6-*t*-Bu<sub>3</sub>C<sub>6</sub>H<sub>2</sub>)<sub>2</sub>·2PMe<sub>3</sub>, is a distorted tetrahedral structure with O–Zn–O and P–Zn–P bond angles of 108.8(2)° and 107.1(9)°, respectively. Competitive phosphine binding studies monitored by <sup>31</sup>P NMR spectroscopy provided a relative binding order of PPh<sub>3</sub> ≈ P<sup>*t*</sup>Bu<sub>3</sub> << PPh<sub>2</sub>Me < PCy<sub>3</sub> < PMe<sub>2</sub>Ph < PnBu<sub>3</sub> < PEt<sub>3</sub> < PMe<sub>3</sub>. Hence, the relative binding of basic phosphine ligands at these congested zinc sites is largely determined by their steric requirements. All phosphine adducts, with the exception of PMe<sub>2</sub>Ph and PMe<sub>3</sub>, were found to undergo slow self-exchange (<600 s<sup>-1</sup>) with free phosphine by <sup>31</sup>P NMR spectroscopy. However, the two small phosphines, PMe<sub>2</sub>Ph (cone angle = 122°) and PMe<sub>3</sub> (cone angle = 118°), were shown to undergo rapid exchange presumably via an associative mechanism. Although there was no kinetic preferences for PCy<sub>3</sub> binding to cadmium vs zinc, cadmium was thermodynamically favored by about a factor of 2.5. The addition of up to 3 equiv of PCy<sub>3</sub> to the Zn(O-2,4,6-*t*-Bu<sub>2</sub>C<sub>6</sub>H<sub>3</sub>)<sub>2</sub> or Zn(O-2,4,6-*t*-Bu<sub>3</sub>C<sub>6</sub>H<sub>2</sub>)<sub>2</sub> derivatives did not significantly alter the reactivity of these catalysts for the copolymerization of cyclohexene oxide (CHO) and CO<sub>2</sub> to high-molecular weight poly(cyclohexene carbonate). However, the presence of PCy<sub>3</sub> greatly retarded their ability to homopolymerize CHO to polyether or to afford polyether linkages during the copolymerization of CHO/CO<sub>2</sub>.

## Introduction

A focus of our current research interest is the coupling of CO<sub>2</sub> and epoxides to produce polycarbonates catalyzed via zinc complexes such as (2,6-diphenylphenoxide)<sub>2</sub>Zn(THF)<sub>2</sub>.<sup>1,2</sup> Other closely related contributions to this area involving isolated zinc complexes have recently been reported.<sup>3–5</sup> Specifically, the process depicted in eq 1 is under investigation because copolymerization is highly favored over cyclic carbonate production in this instance. Nevertheless, polyether formation still occurs and remains a process we wish to minimize in all CO<sub>2</sub>/epoxide copolymerization reactions.



<sup>†</sup> Dedicated to Professor Heinrich Vahrenkamp on the occasion of his 60th birthday.

- (1) Darensbourg, D. J.; Holtcamp, M. W. *Macromolecules* **1995**, *28*, 7577.
- (2) Darensbourg, D. J.; Holtcamp, M. W.; Struck, G. E.; Zimmer, M. S.; Niezgoda, S. A.; Rainey, P.; Robertson, J. B.; Draper, J. D.; Reibenspies, J. H. *J. Am. Chem. Soc.* **1999**, *121*, 107.
- (3) Super, M.; Berluce, E.; Costello, C.; Beckman, E. *Macromolecules* **1997**, *30*, 368.

Because the copolymerization process appears to proceed via an anionic coordinative mechanism, it is of interest to examine the binding of various donor ligands at the active metal site.<sup>6</sup> Organophosphines have long been exploited in homogeneous catalysis as ancillary ligands because of the ability to systematically vary the substituents on the phosphorus and, hence, the steric and electronic properties of the phosphine.<sup>7–14</sup> In addition, we wish to assess the influence of phosphine ligands on the reactivity of the metal center with regard to the CO<sub>2</sub>/epoxide coupling reaction depicted in eq 1. Relevant to these studies,

- (4) Super, M.; Beckman, E. J. *Macromol. Symp.* **1998**, *127*, 89.
- (5) Cheng, M.; Lobkovsky, E. B.; Coates, G. W. *J. Am. Chem. Soc.* **1998**, *120*, 11018.
- (6) Darensbourg, D. J.; Niezgoda, S. A.; Holtcamp, M. W.; Draper, J. D.; Reibenspies, J. H. *Inorg. Chem.* **1997**, *36*, 2426.
- (7) Tolman, C. A. *Chem. Rev.* **1977**, *77*, 313.
- (8) Rahman, Md. M.; Liu, H. Y.; Prock, A.; Giering, W. P. *Organometallics* **1987**, *6*, 650.
- (9) Brown, T. L. *Inorg. Chem.* **1992**, *31*, 1286.
- (10) Grubbs, R. H.; Nguyen, S. T.; Ziller, J. W. *J. Am. Chem. Soc.* **1993**, *115*, 9858.
- (11) Cole Hamilton, D. J.; MacDougall, J. K.; Simpson, M. C.; Green, M. J. *J. Chem. Soc., Dalton Trans.* **1996**, 1161.
- (12) Casey, C. P.; Paulsen, E. L.; Beuttenmueller, E. W.; Proft, B. R.; Petrovich, L. M.; Matler, B. A.; Powell, D. R. *J. Am. Chem. Soc.* **1997**, *119*, 11817.
- (13) Osborn, J. A.; Schrock, R. R. *J. Am. Chem. Soc.* **1976**, *98*, 2134.
- (14) Farnetti, E.; Kaspar, J.; Spogliarish, R.; Gragiani, M. *J. Chem. Soc., Dalton Trans.* **1988**, 947.

phosphine derivatives of zinc are rather rare with most investigations focusing on  $^{31}\text{P}$  NMR studies of phosphine derivatives of zinc halides.<sup>15,16</sup> Crystallographically characterized examples are limited to the chemical vapor deposition (CVD) candidates  $\text{Zn}(\text{S}-2,4,6\text{-t-Bu}_3\text{C}_6\text{H}_3)_2(\text{Ph}_2\text{PMe})$ ,<sup>17</sup>  $(\text{Et}_2\text{NCS}_2)_2\text{Zn}(\text{PMe}_3)$ ,<sup>18</sup> and the zinc halide structure  $[\text{ZnI}_2(\text{PET}_3)]_2$ .<sup>19</sup> Herein, we present the synthesis, solid-state, and solution structures of phosphine adducts of active catalysts for the copolymerization of cyclohexene oxide and  $\text{CO}_2$ , (bisphenoxide)zinc complexes.<sup>20</sup>

## Experimental Section

**Methods and Materials.** All syntheses and manipulations were carried out on a modified Schlenk line or in a glovebox under argon. Glassware was flamed out thoroughly before use. Toluene, hexane, and benzene were freshly distilled from sodium benzophenone, and dichloromethane was distilled from  $\text{P}_2\text{O}_5$  prior to their use. Diphenylmethylphosphine and bisdicyclohexylphosphinomethane were purchased from Strem and stored in a glovebox. Trimethylphosphine was purchased from Aldrich and stored in a Schlenk tube under an atmosphere of argon. Triethylphosphine and tricyclohexylphosphine were purchased from Aldrich and were stored in a glovebox. Tri-*n*-butylphosphine (>90% purity) was purchased from Aldrich packaged as a sure-seal container and was stored under argon atmosphere. All phosphines were used without further purification. The phenols 2,6-di-*tert*-butylphenol, 2,6-diphenylphenol, 2,4,6-trimethylphenol, and 2,4,6-tri-*tert*-butylphenol were all purchased from Aldrich. The 2,4,6-tri-*tert*-butylphenol is very hygroscopic and was purified by means of sublimation in vacuo before use (bath temperature ca. 100 °C, 3.5 mmHg).  $\text{Zn}[\text{N}(\text{SiMe}_3)_2]_2$  was prepared according to the published procedure and isolated through distillation in vacuo as a clear, slightly viscous liquid (bp = 103–104 °C, 4 mmHg).<sup>16</sup> This material is extremely moisture-sensitive and, as such, was stored in a glovebox and used immediately after removal from the box.  $^{31}\text{P}$  NMR data were acquired on Varian XL200 and Unity+ 300 MHz superconducting NMR spectrometers operating at 81 and 121 MHz, respectively. Both instruments are equipped with variable-temperature control modules. All  $^{31}\text{P}$  NMR data are referenced to  $\text{H}_3\text{PO}_4$  (85% in  $\text{D}_2\text{O}$ ).  $^1\text{H}$  and  $^{13}\text{C}$  NMR spectra were acquired on Varian XL200E, Unity+ 300 MHz, and VXR 300 MHz superconducting NMR spectrometers. The operating frequencies for  $^{13}\text{C}$  experiments were 50.29 and 75.41 MHz for the 200 and 300 MHz instruments, respectively. Infrared spectra were recorded on a Mattson 6021 FT-IR spectrometer with DTGS and MCT detectors.

**Synthesis of  $\text{Zn}(\text{O}-2,6\text{-t-Bu}_2\text{C}_6\text{H}_3)_2(\text{PPh}_2\text{Me})$  (1).** To  $\text{Zn}[\text{N}(\text{SiMe}_3)_2]_2$  (0.195 g, 0.5 mmol) in 5 mL of toluene was added a 5 mL toluene solution of 2,6-di-*tert*-butylphenol (0.206 g, 1 mmol). The mixture was stirred for 15 min followed by the addition of  $\text{PPh}_2\text{Me}$  (0.10 g, 0.5 mmol) via a syringe. Stirring of the reaction solution was continued for an additional 30 min, and then the solution was concentrated in vacuo to approximately 2–3 mL. Crystals were obtained through slow diffusion of hexane into the toluene reaction at –20 °C over several days. The yield after drying was 0.16 g (48%). Anal. Calcd for  $\text{ZnC}_4\text{H}_5\text{O}_2\text{P}$ : C, 71.1; H, 8.15. Found: C, 72.85; H, 8.14.  $^1\text{H}$  NMR ( $\text{CD}_2\text{Cl}_2$ ):  $\delta$  1.25 (d,  $J_{\text{P-H}} = 6.8$  Hz, 3H,  $\text{PCH}_3$ ), 1.61 (s, 18H,  $\text{C}(\text{CH}_3)_3$ ), 6.8–7.2 (m, 16H, Ph), 7.38 (d, 2H, *p*- $\text{C}_6\text{H}_3$ ).  $^{13}\text{C}$  NMR ( $\text{CD}_2\text{Cl}_2$ ):  $\delta$  31.92 ( $\text{C}(\text{CH}_3)_3$ ), 35.93 ( $\text{PCH}_3$ ), 165.64 (*ipso*- $\text{C}_6\text{H}_3$ ).  $^{31}\text{P}$  NMR ( $\text{CD}_2\text{Cl}_2$ ):  $\delta$  –19.9.

Syntheses of the other monophosphine derivatives of  $\text{Zn}(\text{O}-2,6\text{-t-Bu}_2\text{C}_6\text{H}_3)_2$  were accomplished in a manner analogous to that described for complex 1.

(15) Goel, R. G.; Henry, W. P.; Jha, N. K. *Inorg. Chem.* **1982**, *21*, 2551.

(16) Goel, R. G.; Ogiini, W. O. *Inorg. Chem.* **1977**, *16*, 1968.

(17) Bochmann, M.; Bwembya, G. C.; Grinter, R.; Powell, A. K.; Webb, K.; Hursthouse, M. B.; Abdul-Malik, K. M.; Magid, M. A. *Inorg. Chem.* **1994**, *33*, 2290.

(18) Zeng, D.; Hampden-Smith, M. J.; Alam, T. M.; Rheingold, A. L. *Polyhedron* **1994**, *13*, 2715.

(19) McAuliffe, C. A.; Bricklebank, N.; Godfrey, S. M.; Mackie, A. G.; Pritchard, R. G. *J. Chem. Soc., Chem. Commun.* **1992**, 944.

(20) Darensbourg, D. J.; Zimmer, M. S.; Rainey, P.; Larkins, D. L. *Inorg. Chem.* **1998**, *37*, 2852.

**$\text{Zn}(\text{O}-2,6\text{-t-Bu}_2\text{C}_6\text{H}_3)_2(\text{PCy}_3)$  (2).** Crystals of **2** were grown from the concentrated toluene solution overnight at 0 °C, providing 0.19 g (54%) of the product. Anal. Calcd for  $\text{ZnC}_6\text{H}_7\text{O}_2\text{P}$ : C, 72.6; H, 9.88. Found: C, 73.1; H, 9.90.  $^1\text{H}$  NMR ( $\text{C}_6\text{D}_6$ ):  $\delta$  0.8–2 (m, 33H,  $\text{PC}_6\text{H}_{11}$ ), 1.77 (s, 18H,  $\text{CCH}_3$ ), 6.81 (t, 2H, *p*- $\text{C}_6\text{H}_3$ ).  $^{13}\text{C}$  NMR ( $\text{C}_6\text{D}_6$ ):  $\delta$  27.6–32 ( $\text{PC}_6\text{H}_{11}$ ), 32.5, 165.2 (*ipso*  $\text{C}_6\text{H}_3$ ).  $^{31}\text{P}$  NMR ( $\text{C}_6\text{D}_6$ ):  $\delta$  7.74.

**$\text{Zn}(\text{O}-2,6\text{-t-Bu}_2\text{C}_6\text{H}_3)_2(\text{PMe}_3)$  (3).** After the volatiles were removed under vacuum, the material was washed twice with cold hexanes, resulting in a white powdery solid in 47% isolated yield.  $^1\text{H}$  NMR:  $\delta$  0.252 (d,  $J_{\text{P-H}} = 8.7$  Hz,  $\text{PCH}_3$ ), 1.66 (s, 18H,  $\text{CCH}_3$ ), 6.81 (t, 2H, *p*- $\text{C}_6\text{H}_3$ ), 7.33 (d, 4H, *m*- $\text{C}_6\text{H}_3$ ).  $^{13}\text{C}$  NMR ( $\text{C}_6\text{D}_6$ ):  $\delta$  10.95 (d,  $J_{\text{P-C}} = 24.2$  Hz), 30.36 ( $\text{CCCH}_3$ ), 31.77 ( $\text{CCH}_3$ ), 115.89, 125.29, 138.82, 165.33 (*ipso*- $\text{C}_6\text{H}_3$ ).  $^{31}\text{P}$  NMR ( $\text{C}_6\text{D}_6$ ):  $\delta$  –48.9.

**$\text{Zn}(\text{O}-2,6\text{-t-Bu}_2\text{C}_6\text{H}_3)_2(\text{PET}_3)$  (4).** A microcrystalline material grew from a toluene solution that had been concentrated down to about 2 mL. The final yield after drying was 0.11 g (37%).  $^1\text{H}$  NMR ( $\text{C}_6\text{D}_6$ ):  $\delta$  0.98 (m, 9H,  $\text{PCH}_2\text{CH}_3$ ), 1.22 (m, 6H,  $\text{PCH}_2\text{CH}_3$ ), 6.92 (t, 2H, *p*- $\text{C}_6\text{H}_3$ ), 7.37 (d, 4H, *m*- $\text{C}_6\text{H}_3$ ).  $^{31}\text{P}$  NMR ( $\text{C}_6\text{D}_6$ ):  $\delta$  –14.0.

**$\text{Zn}(\text{O}-2,6\text{-t-Bu}_2\text{C}_6\text{H}_3)_2(\text{PBu}_3)$  (5).** A white powdery solid (0.137 g, 81% yield) was left behind after the material was washed twice in cold hexanes.  $^1\text{H}$  NMR ( $\text{C}_6\text{D}_6$ ):  $\delta$  0.67–1.23 (m, 9H, PBu), 1.72 (s, 18H,  $\text{CCH}_3$ ), 6.803 (t, 2H, *p*- $\text{C}_6\text{H}_3$ ), 7.33 (d, 4H, *m*- $\text{C}_6\text{H}_3$ ).  $^{13}\text{C}$  NMR ( $\text{C}_6\text{D}_6$ ):  $\delta$  13.42, 20.64 (d,  $\text{PCH}_2$ ), 24.34, 24.52, 115.74, 125.09, 138.70, 165.09 (*ipso*- $\text{C}_6\text{H}_3$ ).  $^{31}\text{P}$  NMR ( $\text{C}_6\text{D}_6$ ):  $\delta$  –21.0.

**Synthesis of  $[\text{Zn}(\text{O}-2,6\text{-t-Bu}_2\text{C}_6\text{H}_3)_2]_2(\text{PCy}_2)_2\text{CH}_2$  (6).** Bisdicyclohexylphosphinomethane (0.1 g, 0.00025 mol) and 2,6-di-*tert*-butylphenol (0.206 g, 0.0005 mol) were dissolved in 5 mL of toluene. The toluene solution was then added to neat  $\text{Zn}[\text{N}(\text{SiMe}_3)_2]_2$  and was stirred for 0.5 h. The volatiles were then stripped away in vacuo, giving a slightly yellowed fine powder in 82% yield.  $^{31}\text{P}$  NMR ( $\text{C}_6\text{D}_6$ ):  $\delta$  –3.77.

**$[\text{Zn}(\text{O}-2,6\text{-t-Bu}_2\text{C}_6\text{H}_3)_2]_2(\text{Me}_2\text{PPh})$  (7).** After the volatiles were removed under vacuum, the product was washed several times with cold hexanes to provide a white powdery solid in 52% yield.  $^1\text{H}$  NMR ( $\text{C}_6\text{H}_6$ ):  $\delta$  0.72 (d,  $\text{PCH}_3$ ), 1.64 (s, 18H,  $\text{CCH}_3$ ), 6.89 (t, 2H, *p*- $\text{C}_6\text{H}_3$ ), 7.37 (d, 4H, *m*- $\text{C}_6\text{H}_3$ ).  $^{31}\text{P}$  NMR ( $\text{C}_6\text{H}_6$ ):  $\delta$  –35.8.

**Synthesis of  $\text{Zn}(\text{O}-2,4,6\text{-t-Bu}_3\text{C}_6\text{H}_3)_2(\text{PMe}_3)$  (8).** A 5 mL toluene solution of 2,4,6-tri-*tert*-butylphenol (0.33 g, 1.3 mmol) was added to  $\text{Zn}[\text{N}(\text{SiMe}_3)_2]_2$  (0.25 g, 0.65 mmol) dissolved in 3 mL of toluene. After the solution was stirred for 30 min, 1 equiv of trimethylphosphine (0.134  $\mu\text{L}$ , 0.65 mmol) was added via a syringe. The mixture was stirred for an extra 15 min and then concentrated down to 1–2 mL. A second equivalent of the phosphine was then added. Very large block crystals of the product grew from the solution overnight at –20 °C. The overall yield was 0.96 g (20%).

**Synthesis of  $\text{Zn}(\text{O}-2,6\text{-Ph}_2\text{C}_6\text{H}_3)_2(\text{Ph}_2\text{PMe})$  (9).** 2,6-Diphenylphenol (0.12 g, 1 mmol) in 5 mL of toluene was added to  $\text{Zn}[\text{N}(\text{SiMe}_3)_2]_2$  (0.195 g, 0.5 mmol) dissolved in 3 mL of toluene. The mixture was stirred for 30 min followed by addition of  $\text{Ph}_2\text{PMe}$ . After the mixture was stirred for an additional 30 min, the volatiles were pulled away in vacuo, leaving behind a tacky, foamy solid. The material was stirred in cold hexane and filtered, giving 0.28 g (73%) of the white powdery product.  $^1\text{H}$  NMR ( $\text{CD}_2\text{Cl}_2$ ):  $\delta$  3.24 (d, 3H), 6.4–7.4 (m, 36H, phenyl).  $^{13}\text{C}$  NMR ( $\text{CD}_2\text{Cl}_2$ ):  $\delta$  55.2 ( $\text{PCH}_3$ ), 115.3, 121.1, 126, 128.2, 128.5, 128.9, 129.1, 129.3, 132.1, 138, 141.9.  $^{31}\text{P}$  NMR ( $\text{CD}_2\text{Cl}_2$ ):  $\delta$  0.29.

**Synthesis of  $\text{Zn}(\text{O}-2,6\text{-Ph}_2\text{C}_6\text{H}_3)_2(\text{PCy}_3)$  (10).** Preparation and isolation were very similar to that for **9**. Removal of the toluene in vacuo left a colorless oil. Pentane was added to the oil, and after the mixture was stirred for several minutes, the product was isolated as a white powder in 48% yield.  $^1\text{H}$  NMR ( $\text{C}_6\text{D}_6$ ):  $\delta$  0.8–1.6 (b, 33H,  $\text{PC}_6\text{H}_{11}$ ), 6.58 (t, 2H, *p*- $\text{C}_6\text{H}_3$ ), 6.85–7.5 (b, 22H, Ph).  $^{13}\text{C}$  NMR ( $\text{C}_6\text{D}_6$ ):  $\delta$  26.1, 27.3 (d), 29.3, 30.5 (d), 116, 123.2, 142, 160.5 (*ipso*).  $^{31}\text{P}$  NMR ( $\text{C}_6\text{D}_6$ ):  $\delta$  12.2.

**Synthesis of  $\text{Zn}(\text{O}-2,6\text{-Ph}_2\text{C}_6\text{H}_3)_2(\text{PMe}_3)$  (11).** Complex **11** was made in a fashion analogous to that of **9** and isolated as a solid in 57% yield.  $^1\text{H}$  NMR ( $\text{C}_6\text{D}_6$ ):  $\delta$  –0.49 (d, 9H,  $J_{\text{P-H}} = 14.1$ ), 6–7.35 (m, 14H), 7.812 (d, 4H, *m*- $\text{C}_6\text{H}_3$ ).  $^{31}\text{P}$  NMR ( $\text{C}_6\text{D}_6$ ):  $\delta$  –47.4.

**Synthesis of  $\text{Zn}(\text{O}-2,6\text{-Ph}_2\text{C}_6\text{H}_3)_2(\text{PET}_3)$  (12).** The synthesis was similar to that for **9** and isolated in 32% yield.  $^1\text{H}$  NMR ( $\text{C}_6\text{D}_6$ ):  $\delta$  0.42 (m, 3H,  $\text{PCH}_2\text{CH}_3$ ), 0.63 (m, 2H,  $\text{PCH}_2\text{CH}_3$ ), 6.87 (t, 2H), 7.39 (d, 4H, *o*- $\text{C}_6\text{H}_3$ ), 7.86 (d, 4H, *m*- $\text{C}_6\text{H}_3$ ).  $^{31}\text{P}$  NMR ( $\text{C}_6\text{D}_6$ ):  $\delta$  –12.1 (b).

**Table 1.** Crystallographic Data and Data Collection Parameters for Complex **8**

formula	C <sub>42</sub> H <sub>76</sub> O <sub>2</sub> P <sub>2</sub> Zn
fw	740.34
cryst system	monoclinic
space group	P2 <sub>1</sub> /c
a, Å	18.271(4)
b, Å	14.648(3)
c, Å	18.930(4)
β, deg	117.06
V, Å <sup>3</sup>	4511.9(16)
Z	4
d(calcd), g/cm <sup>3</sup>	1.090
abs coeff, mm <sup>-1</sup>	1.639
goodness of fit <sup>a</sup> on F <sup>2</sup>	1.069
λ, Å	1.541 84
T, K	193(2)
R, <sup>b</sup> %	6.83
R <sub>w</sub> , <sup>c</sup> %	14.53

<sup>a</sup> GOF =  $[\sum([w(F_o^2 - F_c^2)]^2)/(n - p))]^{1/2}$ , where  $n$  = no. of data and  $p$  = no. of parameters. <sup>b</sup>  $R = \sum(|F_o| - |F_c|)/\sum F_o$ . <sup>c</sup>  $R_w = \{[\sum w(F_o^2 - F_c^2)^2]/[\sum w(F_o^2)^2]\}^{1/2}$ .

**Synthesis of Zn(O-2,6-Ph<sub>2</sub>C<sub>6</sub>H<sub>3</sub>)<sub>2</sub>(PBU<sub>3</sub>) (13).** Complex **13** was made in a fashion analogous to that of **9** and isolated in 22% yield. The product was a sticky colorless solid. <sup>1</sup>H NMR (C<sub>7</sub>D<sub>8</sub>): δ 0.74 (m, 7H, PCH<sub>2</sub>CH<sub>3</sub>), 1.30 (p, 2H, PCH<sub>2</sub>), 6.7–7.5 (m, 22H, Ph), 7.83 (b, 4H, *m*-C<sub>6</sub>H<sub>3</sub>). <sup>31</sup>P NMR (C<sub>7</sub>D<sub>8</sub>): δ -18.6 (b).

**Synthesis of Zn(O-2,4,6-trimethyl-C<sub>6</sub>H<sub>2</sub>)<sub>2</sub>(PMe<sub>3</sub>)<sub>2</sub> (14).** To Zn-[N(SiMe<sub>3</sub>)<sub>2</sub>]<sub>2</sub> (0.095 g, 0.25 mmol) in 5 mL of toluene was added 2,4,6-trimethylphenol (0.068 g, 0.5 mmol) as a toluene solution dropwise over the course of several minutes. After approximately 20% of the phenol had been added, a white solid began to precipitate. The remaining phenol was added and the mixture stirred for an additional 30 min. PMe<sub>3</sub> (0.052 mL, 0.5 mmol) was then added via a syringe. The solution cleared almost instantaneously as a reaction took place. The mixture was then stirred for 10 more minutes. While the toluene was removed in vacuo, the PMe<sub>3</sub> was also evacuated and the material reprecipitated and could not be redissolved in any common solvent.

**Synthesis of Zn(O-2,4,6-trimethyl-C<sub>6</sub>H<sub>2</sub>)<sub>2</sub>(PBU<sub>3</sub>)<sub>2</sub> (15).** Complex **15** was made in a manner similar to that used for **14**. Removal of the toluene left a moist white solid that did not appear to dry further when left under vacuum for an extended period of time. <sup>31</sup>P NMR (C<sub>6</sub>D<sub>6</sub>): δ -31.5 (free PBU<sub>3</sub>), -21.0 (bound PBU<sub>3</sub>), 63.0 (bound PBU<sub>3</sub>(O)).

**Phosphine Competition Studies.** A sample of pure Zn(O-2,6-<sup>t</sup>Bu<sub>2</sub>C<sub>6</sub>H<sub>3</sub>)<sub>2</sub>(PCy<sub>3</sub>), crystallized from a concentrated toluene solution, was dissolved in CD<sub>2</sub>Cl<sub>2</sub> and added to an NMR tube in a glovebox. An equimolar amount of the appropriate phosphine was added via a syringe with vigorous shaking to ensure complete dissolution of the phosphine. <sup>31</sup>P NMR data were recorded at -80, -60, -40, -20, 0, and 20 °C. Ordering of the phosphine affinities was established on the basis of the amount of PCy<sub>3</sub> displaced from zinc.

**Zinc/Cadmium Competition Study.** The synthesis and isolation of Zn(O-2,6-<sup>t</sup>Bu<sub>2</sub>C<sub>6</sub>H<sub>3</sub>)<sub>2</sub>(THF)<sub>2</sub> and its cadmium analogue were carried out as described earlier. To a solution of CD<sub>2</sub>Cl<sub>2</sub> was added a pure sample of Cd(O-2,6-<sup>t</sup>Bu<sub>2</sub>C<sub>6</sub>H<sub>3</sub>)<sub>2</sub>(THF)<sub>2</sub> (0.019 mmol) and an equimolar amount of pure Zn(O-2,6-<sup>t</sup>Bu<sub>2</sub>C<sub>6</sub>H<sub>3</sub>)<sub>2</sub>(THF)<sub>2</sub>. The contents were placed in an NMR tube and cooled to -78 °C. To a separate tube was added 0.019 mmol of PCy<sub>3</sub> in a 1 mL solution of CD<sub>2</sub>Cl<sub>2</sub>. This solution was also cooled to -78 °C. After several minutes at -78 °C, the metal complex mixture was cannulated into the phosphine-containing tube. The entire mixture was maintained at -78 °C and then warmed slowly as <sup>31</sup>P NMR data were acquired at 20 °C temperature increments.

**NOTE!** Cadmium and its complexes are extremely toxic and should be handled with caution. Cadmium waste products should be stored in a separate, clearly marked container.

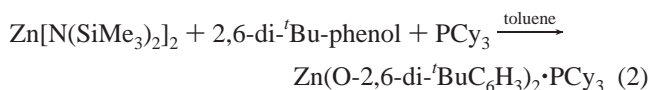
**X-ray Crystallography.** Crystal data and details of the data collections are provided in Table 1. A colorless block crystal of **8** was mounted on a glass fiber with epoxy cement at room temperature and cooled to 163 K (**8**) in a N<sub>2</sub> stream. Preliminary examination and data

collection were performed on a Rigaku AFC5 X-ray diffractometer (Cu Kα, λ = 1.541 78 Å radiation). Cell parameters were calculated from the least-squares fitting of the setting angles for 25 reflections. ω scans for several intense reflections indicated acceptable crystal quality. Data were collected for 8.0° ≤ 2θ ≤ 120°. Three control reflections collected for every 97 reflections showed no significant trends. Lorentz and polarization corrections were applied as was a semiempirical absorption correction to each. Structures were solved by direct methods [SHELXS, SHELXTL-PLUS program package, Sheldrick (1993)]. Full-matrix least-squares anisotropic refinement for all non-hydrogen atoms yielded R, R<sub>w</sub>(F<sup>2</sup>), and S values at convergence. Hydrogen atoms were placed at idealized positions with isotropic thermal parameters fixed at 0.08. Neutral atom scattering factors and anomalous scattering correction terms were taken from the International Tables for X-ray Crystallography.

**Copolymerizations Reactions.** Polymerization experiments were carried out in a Parr 300 mL autoclave high-pressure reactor equipped with a magnetic stirring unit. Prior to reaction, the autoclave was heated to 80 °C in vacuo overnight to remove trace moisture. An appropriate amount of the catalyst (calculated to 0.013 g of Zn content) was then dissolved in the monomers cyclohexene oxide or propylene oxide. The epoxide solution was introduced into the reactor via an injection port, and the reactor was charged to 800 psi of CO<sub>2</sub> and heated to 80 °C for 60–70 h. Methylene chloride was used to extract the sticky, viscous product from the reactor. The polymer was then precipitated from a large volume of methanol and dried in a vacuum oven.

## Results and Discussion

**Syntheses.** The phosphine adducts of the bisphenoxide derivatives of zinc were all synthesized in an analogous manner. That is, 2 equiv of a di- or trisubstituted phenol was added to a pure sample of (bistrimethylsilylamide)zinc in a small volume of toluene under argon, and the reaction solution was stirred at ambient temperature for several minutes. An amount of 1 or 2 equiv of the appropriate phosphine was then added directly to the in situ prepared bisphenoxide zinc derivative. Alternatively, in the case of solid phosphines such as PCy<sub>3</sub>, the phenol and the phosphine could be added concurrently (as depicted in eq 2) without any changes in the product distribution. Indeed, the phosphine ligands do not appear to interact with the zinc amide starting complex except at low temperature. All of the products were colorless, and any solution color change to pale-yellow or, further, to light-green was indicative of progressive stages of decomposition. Crystallization from a concentrated toluene solution, when possible, proved to be the best method for isolation of the pure product. Purity was assessed by <sup>1</sup>H and <sup>31</sup>P NMR spectroscopies and in selected instances via elemental analyses. With the exception of the small phosphine ligand, PMe<sub>3</sub>, all the derivatives isolated were monoadducts of the bis-(phenoxide)zinc complexes.



Sterically encumbering substituents in the **2** and **6** positions of the aryl ring of the phenoxide ligands bound to zinc have the effect of solubilizing these bisphenoxide derivatives in the absence of phosphines in a variety of media, including hexane, benzene, and methylene chloride. This is a consequence of the bulky phenoxide groups' ability to hinder extensive aggregation through the oxygen lone pairs. On the other hand, complexes derived from 2,4,6-trimethylphenol are insoluble in most common organic solvents because the methyl groups are not sufficiently bulky to avert phenoxide bridging. Indeed, a DFT study of Zn(O-2,6-Me<sub>2</sub>C<sub>6</sub>H<sub>3</sub>)<sub>2</sub> at the B3LYP level of theory has revealed that the complex is stabilized by 48.5 kcal/mol upon



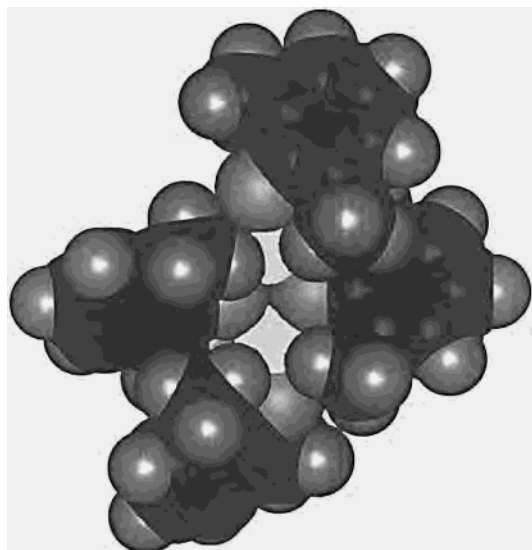


**Figure 1.** Space-filling model of the optimized dimeric structure of  $\{\text{Zn}(\text{O}-2,6\text{-Me}_2\text{C}_6\text{H}_3)_2\}_2$ .

forming the phenoxide-bridged dimer.<sup>21</sup> It has been demonstrated that pyridine is sufficiently basic to disrupt these bridging interactions, and crystals of the complex  $\text{Zn}(\text{O}-2,4,6\text{-Me}_3\text{C}_6\text{H}_2)_2\text{(py)}_2$  have been obtained from a concentrated solution containing a 1:2 mole ratio of zinc phenoxide to pyridine.<sup>2</sup> It has recently come to our attention that the bis-2,6-*t*-Bu<sub>2</sub>-phenoxide zinc derivative crystallizes from hexane as a dimer that has been characterized in the solid-state by X-ray crystallography.<sup>22</sup> Earlier, Caulton and co-workers have reported, on the basis of cryoscopic molecular weight and <sup>1</sup>H NMR measurements in benzene, that the 2,4,6-*t*-Bu<sub>3</sub>-phenoxide zinc derivative crystallized from hexanes was dimeric.<sup>23</sup>

Because of our success at imparting solubility to the  $\{\text{Zn}(\text{O}-2,4,6\text{-Me}_3\text{C}_6\text{H}_2)_2\}_2$  upon addition of pyridine, we anticipated that phosphines would likewise disassemble the aggregate species via  $\sigma$  donation to the metal center. The results were mixed, however, because several phosphine ligands, including  $\text{PPh}_2\text{Me}$  and  $\text{PCy}_3$ , failed to draw the toluene insoluble complex into solution. By contrast, when 2 equiv of  $\text{PMe}_3$  was added to the insoluble dimer, the complex was rapidly solubilized to afford  $\text{Zn}(\text{O}-2,4,6\text{-Me}_3\text{C}_6\text{H}_2)_2\cdot 2\text{PMe}_3$ . Hence, the larger phosphines are incapable of penetrating zinc's sterically hindered inner coordination sphere to affect substitution (see Figure 1 for a space-filling model of the optimized dimeric structure of  $\{\text{Zn}(\text{O}-2,4\text{-Me}_2\text{C}_6\text{H}_3)_2\}_2$ ). Attempted removal of toluene in vacuo from a solution of the bistrimethylphosphine adduct resulted in a reprecipitation of the aggregate species, indicating that the highly volatile  $\text{PMe}_3$  ligand is easily dissociated. Similarly, the less-volatile phosphine *n*-Bu<sub>3</sub>P readily causes the trimethylphenoxide derivative to dissolve in toluene; however, as expected for the less volatile phosphine, the complex remained in solution during the removal of solvent under vacuum.

**Description of Structures.** Previously, we have communicated the solid-state structures of complexes **1** and **2**, the

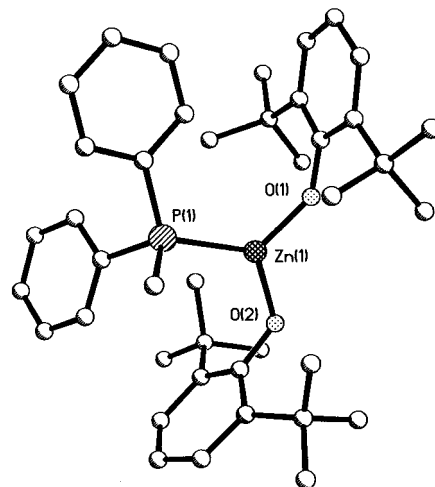


**Figure 2.** Ball-and-stick drawing of complex **1**.

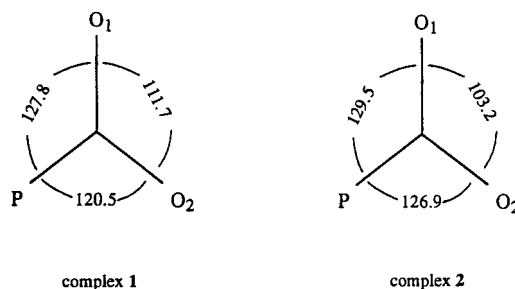


**Figure 3.** Bond angles in the trigonal planes of complexes **1** and **2**.

mono- $\text{PPh}_2\text{Me}$  and  $\text{PCy}_3$  adducts of  $\text{Zn}(\text{O}-2,6\text{-}i\text{-Bu}_2\text{C}_6\text{H}_3)_2$ .<sup>20</sup> One of these structures, complex **1**, is reproduced in a ball-and-stick drawing in Figure 2. These derivatives have a nearly planar arrangement of the zinc center along with the three atoms in its coordination sphere. That is, the zinc atom lies 0.009(2) and 0.070(2) Å out of the plane defined by the phosphorus and two oxygen donor groups for complexes **1** and **2**, respectively. As depicted in Figure 3, the average P–Zn–O angle is larger than the O–Zn–O angle in both instances. The Zn–P bond length in the  $\text{PPh}_2\text{Me}$  derivative at 2.375(2) Å is shorter than that observed in the  $\text{PCy}_3$  adduct of 2.433(2) Å. This is somewhat unexpected because  $\text{PCy}_3$  is the better donating phosphine. Furthermore, the O–Zn–O angle in the  $\text{PCy}_3$  derivative is less obtuse, which would suggest a shorter Zn–P bond length in this instance based on hybridization arguments.<sup>17</sup> Evidently, the difference in Zn–P bond lengths simply can be traced to the larger steric requirement of the tricyclohexylphosphine ligand.

As previously mentioned, when the phosphine ligand is small, it is possible to observe the binding of a second ligand to the parent  $\text{Zn}(\text{O}-2,6\text{-}i\text{-Bu}_2\text{C}_6\text{H}_3)_2$  derivative. For example, upon addition of 2 equiv of  $\text{PMe}_3$  to  $\text{Zn}(\text{O}-2,4,6\text{-}i\text{-Bu}_2\text{C}_6\text{H}_3)_2$ , the bisphosphine adduct was isolated and crystals suitable for X-ray analysis were obtained from toluene at  $-20^\circ\text{C}$ . It was advantageous to synthesize the tri-*tert*-butyl-substituted derivative in this case because of its generally superior crystallization properties. It is noteworthy that Bochmann and co-workers only isolated the mono- $\text{PMe}_3$  adduct of the thiolate analogue of **8** upon reacting  $\{\text{Zn}(\text{S}-2,4,6\text{-}i\text{-Bu}_3\text{C}_6\text{H}_2)_2\}_2$  with 8 equiv of  $\text{PMe}_3$  in hydrocarbon solvent.<sup>17</sup> A thermal ellipsoid drawing of  $\text{Zn}(\text{O}-2,4,6\text{-}i\text{-Bu}_3\text{C}_6\text{H}_2)_2\cdot 2\text{PMe}_3$ , complex **8**, is exhibited in Figure 4. Selected bond lengths and bond angles are provided in Table 2. Comparison of the structural parameters for **8** with those of the copolymerization catalyst,  $\text{Zn}(\text{O}-2,6\text{-}i\text{-Bu}_2\text{C}_6\text{H}_3)_2(\text{THF})_2$ , illustrates the relatively larger steric demands and better donating

(21) Computations were carried out by Dr. Agnes Derecskei-Kovacs in the Laboratory for Molecular Simulations in the Department of Chemistry at Texas A&M University. Detailed results from this study, which includes a variety of alkoxide and aryloxy zinc derivatives, will be published elsewhere.

(22) Kunert, M.; Klobes, O.; Bräuer, M.; Görls, H.; Anders, E.; Dinjus, E. Preceedings of the 1999 SFB Congress, Jena, Germany, p PA2.

(23) Geerts, R. L.; Huffman, J. C.; Caulton, K. G. *Inorg. Chem.* **1986**, *25*, 1803.

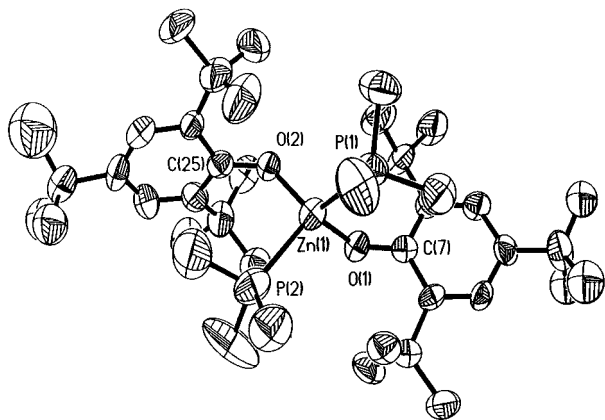


**Figure 4.** Thermal ellipsoid representation of  $\text{Zn}(\text{O}-2,4,6\text{-t-Bu}_3\text{C}_6\text{H}_2)_2 \cdot 2\text{PMe}_3$ , complex **8**.

**Table 2.** Selected Bond Lengths (Å) and Angles (deg) for **8**

Zn(1)–O(1)	1.915(5)	O(2)–C(25)	1.345(8)
Zn(1)–P(1)	2.542(3)	Zn(1)–O(2)	1.923(5)
O(1)–C(7)	1.348(8)	Zn(1)–P(2)	2.588(3)
O(1)–Zn(1)–O(2)	108.8(2)	O(1)–Zn(1)–P(1)	102.1(2)
O(2)–Zn(1)–P(1)	120.3(2)	O(1)–Zn(1)–P(2)	116.8(2)
O(2)–Zn(1)–P(2)	102.7(2)	P(1)–Zn(1)–P(2)	107.01(9)
C(7)–O(1)–Zn(1)	137.3(4)	C(25)–O(2)–Zn(1)	130.1(4)

ability of  $\text{PMe}_3$  vs tetrahydrofuran. First, the average Zn–O bond length of 1.919(5) Å is somewhat longer than that found in the THF-substituted derivative (1.876(5) Å).<sup>2</sup> More significantly, the O–Zn–O bond angle of 108.8(2)° in **8** is considerably less obtuse than the analogous angle in the THF adduct (142.9(2)°). Indeed, this value is more in accord with those observed in the trigonal planar monophosphine derivatives **1** (111.7(2)°) and **2** (103.2(2)°). The O–Zn–P bond angles varied widely from 102.11(16)° for  $\angle\text{O}_1\text{–Zn–P}_1$  to 120.27(15)° for  $\angle\text{O}_2\text{–Zn–P}_1$ . Clearly, the THF derivative assumed a geometry that maximized the separation between the pendant *tert*-butyl groups, whereas **8**, by virtue of its larger and more donating  $\text{PMe}_3$  ligands, conforms to a more symmetrical coordination sphere. At an average of 2.564(3) Å, the Zn–P bond lengths are significantly longer than the analogous bonds in **1** and **2** and longer than the Zn–P distance of 2.413(4) Å found in the  $\text{Zn}(\text{S}-2,4,6\text{-t-Bu}_3\text{C}_6\text{H}_2)_2 \cdot \text{PMe}_3$  adduct. This is as expected on going from three-coordinate zinc to four-coordinate zinc.

**Solution NMR Studies.** We have previously described some preliminary  $^{31}\text{P}$  NMR solution studies of phosphine binding studies to monomeric zinc(II) bisphenoxide complexes containing  $\text{PPh}_2\text{Me}$  (**1**) and  $\text{PCy}_3$  (**2**) as donor ligands.<sup>20</sup> In both derivatives, the phosphines were completely bound to the zinc center in solution at ambient temperature and the exchange with the corresponding free phosphine was slow. That is,  $^{31}\text{P}$  NMR measurements on pure samples of complexes **1** and **2** showed the shifted phosphorus resonances from that of the free phosphine to be temperature-independent over the range 25 to –90 °C in deuterated toluene. Moreover, addition of a second equivalent of the corresponding phosphine produced no discernible changes in the line shape or position of the  $^{31}\text{P}$  resonances of these complexes. Hence, it is safe to conclude that there is no further binding of these phosphines to zinc nor are the phosphine ligands participating in a rapid self-exchange process. On the basis of chemical shift differences, the self-exchange lifetimes of free/bound phosphine must be considerably longer than 1.6 and  $5.9 \times 10^{-3}$  s for complexes **1** and **2**, respectively.

As a continuation of this work, we have compiled  $^{31}\text{P}$  NMR data for a small library of different phosphine–phenoxide

**Table 3.**  $^{31}\text{P}$  NMR Data of  $\text{Zn}(\text{O}-2,6\text{-R}_2\text{C}_6\text{H}_3)_2 \cdot \text{Phosphine}$  Complexes in  $\text{C}_6\text{D}_6$

complex	R substituents (positions)	phosphine	chemical shift, $\delta$ (ppm)	peak position of free ligand (ppm)
<b>1</b>	<i>t</i> -butyl	$\text{Ph}_2\text{PMe}$	–19.9 <sup>a</sup>	–26.6
<b>2</b>	<i>t</i> -butyl	$\text{PCy}_3$	7.74	10.1
<b>3</b>	<i>t</i> -butyl	$\text{PMe}_3$	–47.4	–62.3
<b>4</b>	<i>t</i> -butyl	$\text{PEt}_3$	–14.0	–19.5
<b>5</b>	<i>t</i> -butyl	$\text{PBu}_3$	–21.0	–31.5
<b>6</b>	<i>t</i> -butyl	$\text{Cy}_2\text{PCH}_2\text{PCy}_2$	–3.77	–10.9
<b>7</b>	<i>t</i> -butyl	$\text{Me}_2\text{PPh}$	–35.8	–45.9
<b>9</b>	phenyl	$\text{Ph}_2\text{PMe}$	0.29 <sup>a</sup>	–26.6
<b>10</b>	phenyl	$\text{PCy}_3$	12.2	10.1
<b>11</b>	phenyl	$\text{PMe}_3$	–48.8	–62.3
<b>12</b>	phenyl	$\text{PEt}_3$	–12.1(b)	–19.5
<b>13</b>	phenyl	$\text{PBu}_3$	–18.6(b) <sup>b</sup>	–31.5
<b>15</b>	methyl (2,4,6)	$\text{PBu}_3$	–21.0	–31.5

<sup>a</sup> Measured in  $\text{CD}_2\text{Cl}_2$ . <sup>b</sup> Measured in  $\text{C}_7\text{D}_8$ .

complexes. The phosphorus chemical shift data for complexes **1–7**, **9–13**, and **15**, acquired in  $\text{C}_6\text{D}_6$  or  $\text{CD}_2\text{Cl}_2$  at ambient temperature, are collected in Table 3. From a cursory examination of Table 3 it is evident that the phosphines, which were found to significantly bind to zinc, were all good  $\sigma$  donors with cone angles less than 170°. For example, triphenylphosphine was not shown to afford an adduct with either of the zinc bisphenoxides examined herein. This prerequisite is apparently rather general for zinc derivatives, although numerous examples of cadmium complexes containing the less basic triphenylphosphine ligand are documented in the literature.<sup>24–26</sup> At the same time, the phosphine cannot be too sterically demanding; for example,  $\text{P}^t\text{Bu}_3$ , which has a cone angle of 180°, did not coordinate to the zinc bisphenoxides. The  $^{31}\text{P}$  chemical shifts for the bound phosphine were observed downfield of their respective positions as free ligands, with the exception of the upfield shift noted in complex **2**. Although in some of the bis-(diphenyl phenoxide) derivatives the  $^{31}\text{P}$  NMR signals are broad (e.g., species **12** and **13**), variable temperature measurements from 20 to –80 °C in toluene-*d*<sub>8</sub> showed no indication of phosphine exchange.

Because the  $\text{PMe}_3$  ligand is unique among the phosphines investigated in its reactivity toward the bis(phenoxide)zinc derivatives, affording both mono- and diphosphine adducts, it was of particular interest to examine the FT  $^{31}\text{P}$  NMR spectra of this system. The  $^{31}\text{P}$  spectrum of  $\text{Zn}(\text{O}-2,6\text{-t-Bu}_2\text{C}_6\text{H}_3)_2$  in the presence of 1 equiv of  $\text{PMe}_3$  at ambient temperature displays one resonance in toluene that undergoes a slight downfield shift as the temperature is lowered to –80 °C. In contrast, when 2.1 equiv of  $\text{PMe}_3$  was added to  $\text{Zn}(\text{O}-2,6\text{-t-Bu}_2\text{C}_6\text{H}_3)_2$ , a single, fairly sharp  $^{31}\text{P}$  signal appears at –55.5 ppm that is nearly equidistant from the bound and free positions at –47.4 and –62.3 ppm, respectively (Figure 5). As the temperature is lowered to 0 °C, the  $^{31}\text{P}$  signal begins to migrate downfield. The signal continues to shift downfield and broaden further as the temperature is lowered to –60 °C where coalescence is approached. Below –60 °C, a second small signal surfaces at –62 ppm corresponding to that of the free phosphine. The peaks continue to narrow until, at –90 °C, two sharp peaks are observed at –48.9 and –62.3 ppm. The latter  $^{31}\text{P}$  resonance is due to the slight excess of 2 equiv of  $\text{PMe}_3$  used in the experiment. Hence, this behavior is readily understood in terms of the rapid equilibrium defined by eq 3, with the mono- $\text{PMe}_3$

(24) Cameron, A. F. *J. Chem. Soc. A* **1971**, 1286.

(25) Dakternieks, D. *Aust. J. Chem.* **1982**, 35, 469.

(26) Goel, R. G.; Jha, N. K. *Can. J. Chem.* **1981**, 59, 3267.

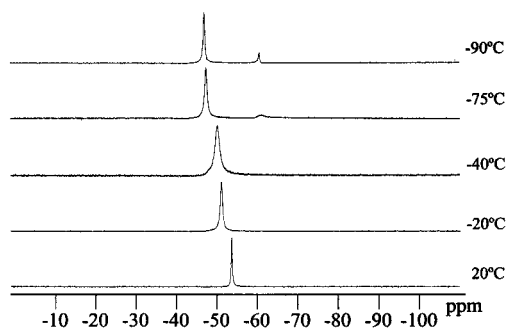
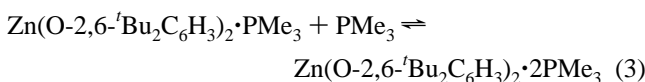


**Figure 5.** Temperature-dependent  $^{31}\text{P}$  NMR spectra of  $\text{Zn}(\text{O}-2,6\text{-}^t\text{Bu}_2\text{C}_6\text{H}_3)_2$  in the presence of 2.1 equiv of  $\text{PMe}_3$ .

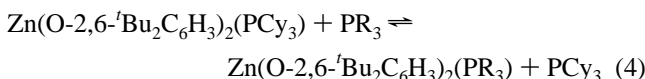
**Table 4.** Integrated Peak Areas of  $^{31}\text{P}$  Signals for Bound and Free  $\text{PEt}_3$  in Reaction 4 as a Function of Temperature

temp ( $^\circ\text{C}$ )	integration areas	
	bound $\text{PEt}_3$	free $\text{PEt}_3$
20	0.42	0.07
0	0.43	0.07
-20	0.44	0.06
-60	0.47	0.03
-80	0.47	0.03

adduct being the primary zinc-containing complex in solution at ambient temperature. As the temperature is lowered to  $-90^\circ\text{C}$ , the equilibrium shifts to the right and the rate of exchange slows to reveal the  $\text{Zn}(\text{O}-2,6\text{-}^t\text{Bu}_2\text{C}_6\text{H}_3)_2\cdot 2\text{PMe}_3$  derivative and free  $\text{PMe}_3$  in the expected ratio of about 20:1 as dictated by the reaction's stoichiometry.



We have expanded these solution studies of bisphenoxide zinc derivatives in the presence of phosphines in order to determine their relative binding affinities. Rapid (NMR time scale) exchange, which occurs via an associative mechanism, has only been noted for the sterically unencumbering  $\text{PMe}_3$  ligand. However, a much slower dissociative route is available to phosphine substitution in this zinc system, which occurs on the time scale of minutes even at low temperatures. These experiments were carried out starting from a pure sample of  $\text{Zn}(\text{O}-2,6\text{-}^t\text{Bu}_2\text{C}_6\text{H}_3)_2(\text{PCy}_3)$ , in the presence of an equimolar quantity of the appropriate phosphine in  $\text{CD}_2\text{Cl}_2$ , and observing the equilibrium position of eq 4 as a function of temperature.



Complex **2** was utilized as the  $\text{Zn}(\text{II})$  source in these studies because it is readily isolable in pure form, thus ensuring a 1:2 stoichiometry of zinc-to-phosphine ligands.

The equilibrium concentrations of the various species (free and zinc-bound phosphine ligands) were determined from the integrated areas of their  $^{31}\text{P}$  resonances. In all instances, equilibrium was established within minutes, since no discernible changes were observed in the  $^{31}\text{P}$  spectra of the mixtures obtained 15 and 45 min following addition of the phosphines. As might be anticipated, there was also not much change in the equilibrium position as a function of temperature as illustrated in Table 4 and Figure 6 for  $\text{PR}_3$  equals  $\text{PEt}_3$ . At  $20^\circ\text{C}$  the amount of bound triethylphosphine was determined to be 86% based on the integration of the peak intensities for the

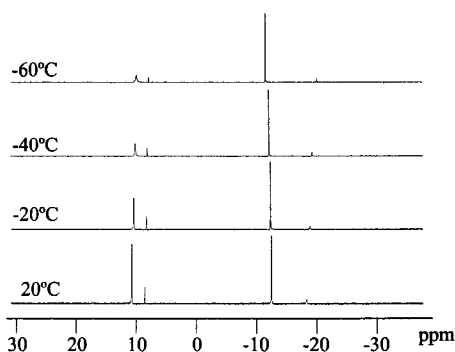


**Figure 6.** Temperature-dependent  $^{31}\text{P}$  NMR spectra of  $\text{Zn}(\text{O}-2,6\text{-}^t\text{Bu}_2\text{C}_6\text{H}_3)_2\cdot\text{PCy}_3$  plus 1 equiv of  $\text{PEt}_3$ .

**Table 5.**  $K_{\text{eq}}$  for Phosphine Exchange Process Defined in Reaction 4<sup>a</sup>

$\text{PR}_3$	$K_{\text{eq}}$	$\Delta G^\circ$ (kcal/mol)
$\text{Ph}_2\text{PMe}$	$9.9 \times 10^{-2}$	1.4
$\text{PEt}_3$	37.7	-2.2
$\text{P}^t\text{Bu}_3$	23.8	-1.9

<sup>a</sup> Measured at ambient temperature.

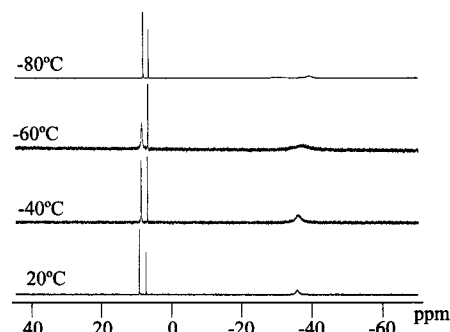


**Figure 7.** Temperature-dependent  $^{31}\text{P}$  NMR spectra of  $\text{Zn}(\text{O}-2,6\text{-}^t\text{Bu}_2\text{C}_6\text{H}_3)_2\cdot\text{PCy}_3$  plus 1 equiv of  $\text{PPhMe}_2$ .

bound and free ligands at  $-13.0$  and  $-19.0$  ppm, respectively. A similar conclusion is reached from the  $^{31}\text{P}$  NMR peak intensities of the bound and free  $\text{PCy}_3$  ligand. Thus, the equilibrium expressed by eq 4 favors the smaller, slightly less basic ( $\text{p}K_{\text{a}}$  of  $\text{PEt}_3 = 8.69$  vs  $9.70$  for  $\text{PCy}_3$ )<sup>27</sup> phosphine.

Relative binding affinities of  $\text{P}^t\text{Bu}_3$  and  $\text{PPh}_2\text{Me}$  vs  $\text{PCy}_3$  were determined in a similar manner. The equilibrium constants measured at ambient temperature for the process depicted in eq 4 are listed in Table 5, along with the respective standard free energy values. An analogous experiment was carried out employing the smaller ligand  $\text{PPhMe}_2$  (cone angle  $122^\circ$ ). However, in this case the zinc-bound  $\text{PMe}_2\text{Ph}$  species present in solution is in rapid equilibrium with free  $\text{PMe}_2\text{Ph}$ , analogous to the *associative* process observed for the other small phosphine,  $\text{PMe}_3$  (vide supra). Figure 7 depicts the temperature-dependent  $^{31}\text{P}$  spectra for this process, where we were unable to freeze out the exchange at  $-80^\circ\text{C}$ . Nevertheless, from the ratio of the  $^{31}\text{P}$  signals for free and bound  $\text{PCy}_3$  it is possible to reason that approximately 75% of the zinc complex is involved in interactions with  $\text{PPhMe}_2$ , which translates into 1.33 equiv of  $\text{PPhMe}_2$  per zinc. Hence, zinc's binding affinity for  $\text{PPhMe}_2$  is slightly greater than that for  $\text{PCy}_3$  but less than that of  $\text{P}^t\text{Bu}_3$  or  $\text{PEt}_3$ . Therefore, if we include the facts that 1 equiv of  $\text{PMe}_3$  completely displaces  $\text{PCy}_3$  from complex **2** and  $\text{PPh}_3$  and  $\text{P}^t\text{Bu}_3$  are not able to displace  $\text{PCy}_3$  from complex **2** to any

(27) Rahman, Md. M.; Liu, H.-Y.; Eriks, K.; Prock, A.; Giering, W. P. *Organometallics* **1989**, *8*, 1.



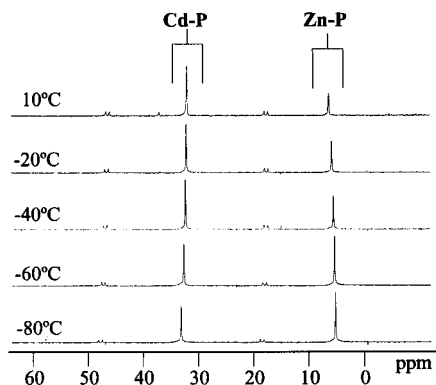
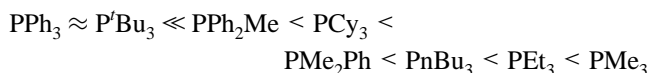


**Figure 8.** Temperature-dependent  $^{31}\text{P}$  NMR spectra of equimolar mixture of  $\text{Cd}(\text{O}-2,6\text{-}t\text{-Bu}_2\text{C}_6\text{H}_3)_2(\text{THF})_2$  and  $\text{Zn}(\text{O}-2,6\text{-}t\text{-Bu}_2\text{C}_6\text{H}_3)_2(\text{THF})_2$  with 1 equiv of  $\text{PCy}_3$  ( $^{113}\text{Cd}-^{31}\text{P}$  and  $^{111}\text{Cd}-^{31}\text{P}$  coupling noted).

measurable extent, the order of phosphine binding affinities to the sterically crowded zinc center in  $\text{Zn}(\text{O}-2,6\text{-}t\text{-Bu}_2\text{C}_6\text{H}_3)_2$  is



In complementary undertakings we have been carrying out comparative structural and reactivity studies of analogous cadmium bis(phenoxide) derivatives to those presented herein involving zinc.<sup>28,29</sup> These investigations have established that, primarily because of its larger size, the chemistry of cadmium is much more diverse when compared to that of zinc. For example, whereas  $\text{Zn}(\text{O}-2,6\text{-}t\text{-Bu}_2\text{C}_6\text{H}_3)_2(\text{THF})_2$  is a distorted tetrahedral structure, its cadmium analogue is square-planar.<sup>15,30</sup> Additionally, the cadmium phenoxide derivative binds three molecules of pyridine, whereas its zinc analogue binds two. In studies directly related to those reported herein, we have shown by  $^{113}\text{Cd}$  NMR that  $\text{Cd}(\text{O}-2,6\text{-}t\text{-Bu}_2\text{C}_6\text{H}_3)_2$  forms only a mono-phosphine adduct with the very large  $\text{PCy}_3$  ligand.<sup>31</sup> On the other hand, the smaller trialkylphosphines such as  $\text{PR}_3$  ( $\text{R} = \text{Me}, \text{Et}, ^t\text{Bu}$ ) readily form diadducts. Hence, this system should allow us to demonstrate in a competitive experiment whether there is any kinetic or thermodynamic preference of  $\text{PCy}_3$  for similar Zn/Cd sites.

To this end, an equimolar mixture of  $\text{Cd}(\text{O}-2,6\text{-}t\text{-Bu}_2\text{C}_6\text{H}_3)_2(\text{THF})_2$  and  $\text{Zn}(\text{O}-2,6\text{-}t\text{-Bu}_2\text{C}_6\text{H}_3)_2(\text{THF})_2$  in  $\text{CD}_2\text{Cl}_2$  was added to a solution containing 1 equiv of  $\text{PCy}_3$  at  $-78^\circ\text{C}$ . The reaction's progress was monitored by  $^{31}\text{P}$  NMR spectroscopy, with data collected incrementally over the temperature range  $-80^\circ$  to  $10^\circ\text{C}$  as depicted in Figure 8. The initially observed cadmium to zinc-bound phosphine ratio is quite close to a statistical distribution, thus indicating little kinetic preference of  $\text{PCy}_3$  for cadmium vs zinc. Changes in the product distribution as the temperature of the solution was increased are summarized in Figure 9. In the region between  $-80$  and  $-60^\circ\text{C}$ , where phosphine exchange is expected to be slow, the quantity of cadmium-bound phosphine vs zinc-bound phosphine was unchanged. However, when the mixture was warmed to  $-40^\circ\text{C}$ , a significant increase in the concentration of the cadmium phosphine adduct, with a concomitant decrease in

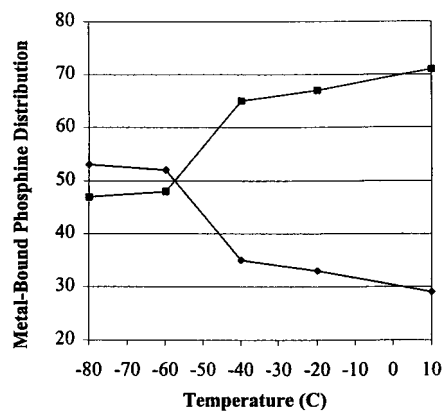


**Figure 9.** Plot of changes in  $[\text{Cd-P}]/[\text{Zn-P}]$  distribution obtained from Figure 8 as the temperature is increased from  $-80$  to  $+10^\circ\text{C}$ : (●) zinc-bound phosphine; (■) cadmium-bound phosphine.

**Table 6.** Zinc Bis(phenoxide)phosphine Catalyzed Copolymerization of  $\text{CHO}/\text{CO}_2$  at  $80^\circ\text{C}$  and 800 psi  $\text{CO}_2$  Pressure<sup>a</sup>

aryl substituents (positions)	phosphine	% carbonate	% conversion <sup>b</sup>	turnovers <sup>c</sup> (g/g of Zn)
$t\text{-Bu}(2,6)$	$\text{PCy}_3$	92	36	806
$t\text{-Bu}(2,6)$	$\text{PCy}_3^d$	95	32	699
$t\text{-Bu}(2,4,6)$	$\text{PCy}_3$	98	39	852
$t\text{-Bu}(2,6)$	$\text{PPh}_2\text{Me}$	93	11	240

<sup>a</sup> Reactions were carried out for about 62 h. <sup>b</sup> Calculated via integration of the  $^1\text{H}$  NMR peak intensities for the bulk mixture. <sup>c</sup> Catalyst quantities used contained 0.013 g of Zn. <sup>d</sup> Reaction performed in the presence of additional 2 equiv of  $\text{PCy}_3$ .

its zinc analogue, was observed. This change continued until  $[\text{Cd-P}]/[\text{Zn-P}]$  was about 2.5 at  $10^\circ\text{C}$  with no significant changes occurring beyond this point. Hence, as might have been anticipated, there is a thermodynamic preference for phosphine cadmium binding vs phosphine zinc binding, albeit small. Consistent with the above interpretation, when the temperature of the thermodynamically established equilibrium mixture was lowered, no notable change in the complex distribution was observed.

**Copolymerization of Cyclohexene Oxide (CHO) and Carbon Dioxide.** In this section we examine the effect of addition donor ligands at the zinc center of zinc bis(phenoxides) on their efficacy as catalysts for the copolymerization of  $\text{CHO}/\text{CO}_2$  to poly(cyclohexene carbonate). On the basis of the solution behavior of the various zinc bis(phenoxide) phosphine adducts described above, it is clear that the phosphine ligands, in the presence of weak alternative ligands such as  $\text{CO}_2$  or epoxides, remain bound to the metal center under the conditions of the copolymerization reaction (eq 1). To quantitatively assess the consequence of phosphine ligands on reaction 1 catalyzed by bis( $\text{O}-2,6\text{-}t\text{-Bu}_2\text{C}_6\text{H}_3$ ) $_2\text{Zn}$ , we have employed pure samples of complexes **1** and **2** as catalysts. A summary of our observations is listed in Table 6.

Poly(alkylene)carbonate production in the absence of concurrent polyether formation is a desirable feature of good copolymerization catalysts. In other instances it is beneficial to be able to control the  $\text{CO}_2$  content of the copolymer. Hence, the 2,6-di-*tert*-butylphenoxide and 2,4,6-tri-*tert*-butylphenoxide derivatives of zinc were utilized in these studies because we have previously shown these to produce the largest percentages of polyether linkages (greatest values of  $m$  in eq 1).<sup>1,2</sup> Concomitantly, these zinc complexes are good catalysts for the homopolymerization of  $\text{CHO}$  to poly(cyclohexene oxide). It is immediately evident from the polymer runs in Table 6 that in the presence of  $\text{PCy}_3$ , a strongly binding phosphine to zinc, these

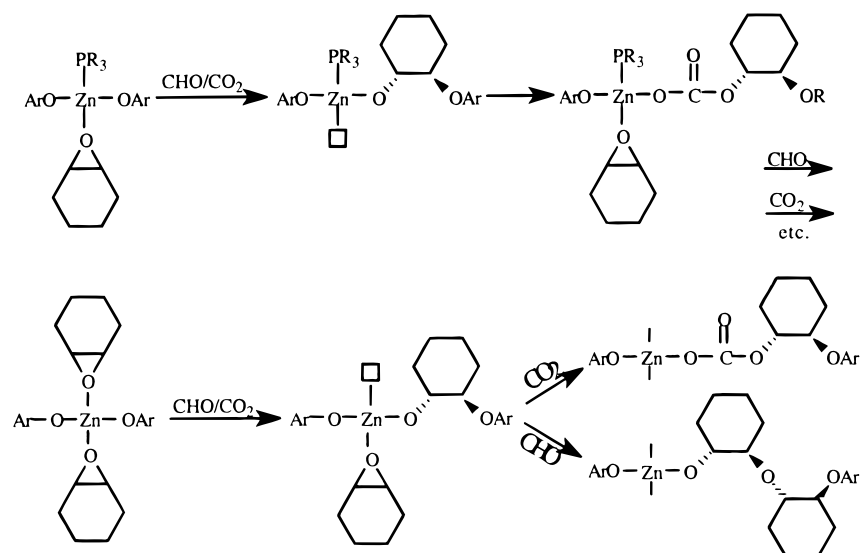
(28) Darensbourg, D. J.; Niezgoda, S. A.; Reibenspies, J. H.; Draper, J. D. *Inorg. Chem.* **1997**, *36*, 5686.

(29) Darensbourg, D. J.; Niezgoda, S. A.; Draper, J. D.; Reibenspies, J. H. *J. Am. Chem. Soc.* **1998**, *120*, 4690.

(30) Goel, S. C.; Chiang, M. Y.; Buhro, W. E. *J. Am. Chem. Soc.* **1990**, *112*, 6724.

(31) Darensbourg, D. J.; Rainey, P.; Larkins, D. L.; Reibenspies, J. *Inorg. Chem.* **2000**, *39*, 473.

Scheme 1



catalysts afford very high percentages of 1:1 copolymers. This is dramatically illustrated for the 2,4,6-tri-*tert*-butylphenoxide derivative (entry 3 in Table 6), which in the absence of  $\text{PCy}_3$  homopolymerizes cyclohexene oxide at ambient temperature. Indeed, to bring about copolymer production with this catalyst (<50% polycarbonate linkages), it was necessary to physically isolate the catalyst from the CHO prior to pressurizing the reactor with  $\text{CO}_2$ , a procedure unnecessary in the presence of  $\text{PCy}_3$ . At the same time the yield of copolymer (or activity of the catalyst) was not greatly affected by the presence of even 3 equiv of  $\text{PCy}_3$  (entry 2). On the other hand, there is some reduction in copolymer yield in the presence of the less basic phosphine  $\text{PPh}_2\text{Me}$ . A similar, albeit less impressive, behavior was noted when  $\text{PPh}_3$  was added to a triethylaluminum catalyst in an early report.<sup>32</sup> Hence, it appears that only one metal binding site is required for copolymerization (recall that  $\text{CO}_2$  insertion does not necessitate prior metal coordination),<sup>33</sup> but two binding sites are needed for consecutive epoxide insertions to be competitive with the very rapid  $\text{CO}_2$  insertion process. This is summarized in Scheme 1. This interpretation is consistent with the observation that  $\text{PMe}_3$ , which is capable of forming a bis(phosphine) adduct with zinc, completely inhibits catalysis. Recent results of Coates and co-workers<sup>5</sup> further confirm this conclusion; that is, in this latter study, by use of a diimine zinc catalyst containing a methoxide or acetate ligand for initiation, no polyether formation was observed. Similarly, the soluble

dimeric species  $\text{Zn}_2(\text{O}-2,6\text{-F}_2\text{C}_6\text{H}_3)_4 \cdot 2\text{THF}$ , which has only one epoxide binding site, effectively catalyzes the copolymerization of CHO and  $\text{CO}_2$  without formation of polyether linkages.<sup>34</sup> Correlatively, the insoluble zinc catalyst systems derived from the reaction of zinc oxide and dicarboxylic acids, which afford significant quantities of polyether linkages, must operate via a zinc center with two vacant sites for substrate binding.<sup>35,36</sup> An additional consideration is that the binding of the weakly basic epoxide ligand to the zinc center may be reduced in the presence of electron-donating phosphine ligands; nevertheless, there is not a significant decrease in the rate of copolymerization in the presence of  $\text{PCy}_3$ . This is amply demonstrated in the observation that the reactivity of  $\text{Zn}(\text{O}-2,4,6\text{-}^t\text{Bu}_3\text{C}_6\text{H}_2)_2$  as a homopolymerization catalyst for CHO is greatly inhibited in the presence of  $\text{PCy}_3$ .

**Acknowledgment.** The financial support of this research by the National Science Foundation (Grant CHE96-15866) and the Robert A. Welch Foundation is greatly appreciated.

**Supporting Information Available:** An X-ray crystallographic file in CIF format for the structure determination of complex **8**. This material is available free of charge via the Internet at <http://pubs.acs.org>. IC990594A

(32) Koinuma, H.; Hirai. *Makromol. Chem.* **1977**, *178*, 1283.

(33) Darensbourg, D. J.; Mueller, B. L.; Bischoff, C. J.; Chojnacki, S. S.; Reibenspies, J. H. *Inorg. Chem.* **1991**, *30*, 2418.

(34) Darensbourg, D. J.; Wildeson, J. R. Unpublished observations.

(35) Soga, K.; Imai, E.; Hattori, I. *Polym. J.* **1981**, *13*, 407.

(36) (a) Rokicki, A. (Air Products and Chemicals, Inc. and Acro Chemical Co.) U.S. Patent 4,943,677, 1990. (b) Motika, S. (Air Products and Chemicals, Inc., Acro Chemical Co., and Mitsui Petrochemical Industries Ltd.) U.S. Patent 5,026,676, 1991.